GRASP: the Future!

Ian Grant[1] and Harry Quiney[2]

1. Oxford University Mathematical Institute, Oxford OX2 6GG, U.K.
2. School of Physics, University of Melbourne, Victoria 3010, Australia

ipg@maths.ox.ac.uk; quiney@unimelb.edu.au

Abstract:
Relativistic atomic and molecular structure calculations start from very different premises to quantum electrodynamics (QED). QED predicts radiative corrections that can only be approximated crudely in today's atomic structure programs. This paper describes rigorous simple algorithms for including accurate vacuum polarization and self-energy corrections in the GRASP programs.

Keywords: relativistic atomic structure; radiative corrections; quantum electrodynamics; numerical methods

1 Introduction

The nonrelativistic ATSP and the relativistic GRASP atomic structure programs have a common origin: the work of Douglas Hartree and his colleagues in the pre-computer era, surveyed in his well-known 1957 lectures. The precursors of the relativistic GRASP program adopted similar computational methods of which there are still traces in the latest version GRASP2018. The dominating spherical symmetry near the atomic nucleus made the finite difference algorithms in ATSP and GRASP useless for modelling molecules. The answer was to adopt the basis set methods of Roothaan and Hall in which the wave functions are expanded in families of simple analytic functions. Relativistic 4-spinor basis sets obeying strict symmetry conditions have been remarkably successful for molecular studies and have revealed insights that led to this paper.

Quantum electrodynamics (QED) was designed as a theory of scattering of the quanta of independent free electron, positron and photon fields. It does not fit well with current atomic and molecular structure programs. QED perturbation theory predicts small corrections to atomic and molecular structure that are difficult to estimate convincingly in GRASP and other programs. This paper demonstrates that CK-spinor basis sets, which feature relativistic symmetry, kinetic matching and charge conjugation symmetry should be considered for future use in GRASP and its molecular generalization BERTHA. Test calculations of vacuum polarization reproduce known results without introducing divergent integrals, suggesting a need to re-evaluate the role of regularization and renormalization in QED.

Preprints (www.preprints.org) | NOT PEER-REVIEWED | Posted: 18 July 2022 doi:10.20944/preprints202207.0266.v1

2 Building atomic structure programs

The software repository [1] of the CompAS (Computational Atomic Structure) collaboration [2] supplies the nonrelativistic ATSP and the relativistic GRASP programs, both based on multiconfiguration Hartree-Fock ideas expounded in Hartree's 1957 lectures [3]. Bound electron orbitals, the building blocks of non-relativistic configurational states (CSF) in ATSP have the familiar form:

$$\psi_{nlm\sigma}(\mathbf{r}) = P_{nl}(r)\, Y_{lm}(\theta,\varphi)\, \phi_\sigma \tag{1}$$
$$l = 0, 1, 2, \ldots, \quad m = l, l-1, \ldots, -l, \quad \sigma = \pm 1/2,$$
$$\varphi_{1/2} = \begin{pmatrix} 1 \\ 0 \end{pmatrix}, \quad \varphi_{-1/2} = \begin{pmatrix} 0 \\ 1 \end{pmatrix}$$

in spherical polar coordinates, where l, m are orbital angular momentum quantum numbers and $\sigma = \pm 1/2$ the spin projection. The label n enumerates successive bound orbitals of this symmetry, replaced by the energy, ε, above threshold for ionization to the continuum. We shall refer to the $2 \times (2l+1)$ orbitals labelled $nlm\sigma$ as the nl-subshell, with the common radial factor $P_{nl}(r)$.

In relativistic programs like GRASP these are replaced by 4-component spinors [4, 5]

$$\psi_{n\kappa m}(\mathbf{r}) = \frac{1}{r} \begin{pmatrix} P_{n\kappa}(r)\chi_{\kappa,m}(\theta,\varphi) \\ iQ_{n\kappa}(r)\chi_{-\kappa,m}(\theta,\varphi) \end{pmatrix}, \tag{2}$$

where the 2-component coupled spin-orbit function is

$$\chi_{\kappa m}(\theta,\varphi) = \sum_{\sigma=\pm 1/2} \langle l, 1/2, j, m \,|\, l, m-\sigma, 1/2, \sigma\rangle\, Y_{l,m-\sigma}(\theta,\varphi)\, \phi_\sigma, \tag{3}$$
$$l = j + \eta/2, \quad \kappa = \eta(j+1/2), \quad (\eta = \pm 1), \quad m = -j, \ldots, j.$$

In this case each $n\kappa$-subshell consists of $2j+1 = 2|\kappa|$ orbitals, with common radial functions $P_{n\kappa}(r)$, $Q_{n\kappa}(r)$. It is often convenient to replace the $n\kappa$ label with the more familiar set $nljm$ with $j = l \pm 1/2$, as $P_{n\kappa} \to P_n l(r)$, and $Q_{n\kappa} \sim O(1/c)$ and vanishes in the limit $c \to \infty$.

These orbital functions are the building blocks for many-electron wave functions. The simplest is the Slater determinant

$$\langle x_1, \ldots, x_n \,|\, j_1, j_2, \ldots, j_n\rangle = \frac{1}{\sqrt{n!}} \begin{vmatrix} \psi_{j_1}(x_1) & \psi_{j_2}(x_1) & \ldots & \psi_{j_n}(x_1) \\ \psi_{j_1}(x_2) & \psi_{j_2}(x_2) & \ldots & \psi_{j_n}(x_2) \\ \vdots & \vdots & \vdots & \\ \psi_{j_1}(x_n) & \psi_{j_2}(x_n) & \ldots & \psi_{j_n}(x_n) \end{vmatrix}, \tag{4}$$

that vanishes if more than one electron orbital is assigned the same state label j_r or the same location x_s, thus ensuring that no orbital has more than one occupant in accordance with Pauli's exclusion principle. GRASP programs classify configurational states (CSF) - notionally a linear combination of Slater determinants - in jj-coupling: $\Phi(\gamma, J^\pi, M)$ denotes an n-electron CSF with total angular momentum quantum numbers J, M, and parity π; γ includes all additional information, in particular the angular momentum coupling scheme, needed to specify $\Phi(\gamma, J^\pi, M)$ uniquely using Racah's theory of angular momentum [5, Sections 6.6-6.8]. CSF in ATSP, $\Phi(\gamma, L, M_L, S, M_S)$, are formed in

Preprints (www.preprints.org) | NOT PEER-REVIEWED | Posted: 18 July 2022 doi:10.20944/preprints202207.0266.v1

much the same way. The atomic state functions, ASFs, are linear combinations of CSFs of the same symmmetry, $\Psi(\Gamma, J^\pi, M) = \sum_\gamma c_{\Gamma\gamma}\, \Phi(\gamma, J^\pi, M)$.

Given estimates of the orbitals, we can construct matrix elements $\boldsymbol{H}_{\gamma\gamma'}$ of the Hamiltonian of an N-electron atom with respect to the CSFs $\Phi(\gamma, J^\pi, M)$. Diagonalization of $\boldsymbol{H}$ generates ASFs $\Psi(\Gamma, J^\pi, M)$ and ASF energies $E(\Gamma, J^\pi)$ with the same spectroscopic classification.

The GRASP orbital equations are described in [5, Chapter 7]. The (unquantized) MCDHFB Hamiltonian for an N-electron atom with point charge nucleus Z has the form

$$H = \sum_{i=1}^{N} (h_i - Z/r_i) + \sum_{i<j} V_{ij}, \tag{5}$$

where

$$h_i = c\boldsymbol{\alpha}_i \cdot \boldsymbol{p}_i + (\beta_i - 1)c^2 \tag{6}$$

is the Dirac Hamiltonian for electron i. The electron-electron interaction potential V_{ij} is just the classical Coulomb potential, augmented by the magnetic Breit interaction. A standard variational argument generates coupled sets of integro-differential equations, one for each participating subshell A, of the form [5, Section 7.3]

$$\begin{bmatrix} -\dfrac{Z_A(r)}{r} - \varepsilon_{AA} & c\left(-\dfrac{d}{dr} + \dfrac{\kappa_A}{r}\right) \\ c\left(\dfrac{d}{dr} + \dfrac{\kappa_A}{r}\right) & -2c^2 - \varepsilon_{AA} - \dfrac{Z_A(r)}{r} \end{bmatrix} \begin{bmatrix} P_A(r) \\ Q_A(r) \end{bmatrix} = -\frac{1}{r} \begin{bmatrix} X_A^+(r) \\ X_A^-(r) \end{bmatrix}. \tag{7}$$

The potential $-Z_A(r)/r$ is the sum of the nuclear Coulomb potential $-Z/r$ and, the 'direct' (or classical) Coulomb repulsion from subshells $B, C, \ldots$; the $X_A^\pm(r)/r$ on the right are 'exchange' potentials[1] together with any Lagrange multipliers, $\varepsilon_{AB}, \ldots$, required to preserve orbital orthonormality. Each such equation, given estimates of the interaction with other subshells, provides an estimate of $P_A(r), Q_A(r)$. They can be used to modify the interaction potentials for the next iteration of the equations until all orbitals have stabilized to agreed precision.

The equations (7) recognize only subshells containing at least one electron, Other one-electron states of that symmetry are ignored, in particular the negative energy solutions representing positrons in the atomic field. These are never calculated in MCDHFB models but, though ignored, they are implicitly part of the model.

Numerical methods to solve the equations (7) in GRASP and similar programs in the Hartree tradition are mostly based on finite differences although a number of recent programs have used B-spline expansions. Relativistic molecular calculations require basis set methods proposed by Roothaan [6] and Hall [7]. This approach has rarely been used for atomic problems, and there were many failed attempts to construct 4-spinor basis sets before the need for kinetic matching of the two radial components was established [5, Sec. 5.7]. The BERTHA

[1] The exchange repulsion energy from other electrons in subshell A is included in $Z_A(r)$

Preprints (www.preprints.org) | NOT PEER-REVIEWED | Posted: 18 July 2022 doi:10.20944/preprints202207.0266.v1

relativistic molecular package [8] relies on the atomic KG-spinor basis sets described in Sec. 3.3.1. Four-spinor basis set algorithms automatically generate both electron and positron wave functions; the positron solutions play no part in atomic and molecular structure. Calculation of additional contributions suggested by QED require a computational scheme with further symmetry constraints on the 4-spinor basis functions to balance the representation of electrons and positrons.

3 QED of atoms and molecules

3.1 Relativistic wave equations

The early history of relativistic wave equations is well documented by, for example, the books [9, 10, 11]. Dirac's sea of 'negative energy states' [12, 13, 14] accompanied by 'hole theory' made it impossible to regard his relativistic wave equation as describing motion of a single particle in the manner of the Schrödinger equation, inspiring the development of quantum field theory. The interpretation of Dirac's 'hole theory' has created major problems in the design of mathematical and computational algorithms for relativistic atomic and molecular structure. Variational methods of nonrelativistic quantum mechanics are routinely justified by the existence of a finite lower bound to the atomic or molecular Hamiltonian, so that iterative decreasing sequences of level energies may converge to a limit according to Cauchy's general principle of convergence. The spectra of Dirac Hamiltonians are infinite above and below; the traditional response has been to assert that variational methods cannot be applied to relativistic atomic and molecular structure problems. This is where relativistic spinor adaptations of the ideas of Roothaan [6] and Hall [7] and an understanding of symmetry constraints came to our aid.

3.2 Quantized electron and positron fields

This section follows [11, Sec. 14.1]. The Dirac equation for *free particles* (in atomic units) is

$$(i\gamma^\mu\partial_\mu - mc)\psi(x) = 0, \quad x = \{x^0, x^1, x^2, x^3\} \equiv (ct, \boldsymbol{x}). \tag{8}$$

We can think of this as a *field equation*, interpreting $\psi(x)$ as an *operator* on the states of the Dirac field rather than providing particle wave functions. Label the states of the Dirac field Φ_n, where the index n runs over all possible field modes, with the *vacuum state* Φ_0. We define the *wave functions* $U_r(x)$, $V_s(x)$ such that

$$U_r(x) = \langle\Phi_0,\, \psi(x)\Phi_r\rangle, \qquad V_s(x) = \langle\Phi_s,\, \psi(x)\Phi_0\rangle \tag{9}$$

as solutions of the equations

$$(i\gamma^\mu\partial_\mu - mc)U_r(x) = 0, \qquad (i\gamma^\mu\partial_\mu - mc)V_s(x) = 0.$$

Invariance with respect to time translation allows us to write

$$U_r(x) = e^{-iE_rt}u_r(\boldsymbol{x}),\ (E_r > 0), \qquad V_s(x) = e^{+iE_st}v_s(\boldsymbol{x}),\ (E_s > 0) \tag{10}$$

Preprints (www.preprints.org) | NOT PEER-REVIEWED | Posted: 18 July 2022 doi:10.20944/preprints202207.0266.v1

for positive and negative energy modes respectively, so that the $\boldsymbol{x}$-dependent amplitudes satisfy the time-independent Dirac equations

$$(c\boldsymbol{\alpha}\cdot\boldsymbol{p}+\beta c^2)u_r(\boldsymbol{x})=E_r u_r(\boldsymbol{x}),\quad (c\boldsymbol{\alpha}\cdot\boldsymbol{p}+\beta c^2)v_s(\boldsymbol{x})=-E_s v_s(\boldsymbol{x}). \tag{11}$$

Expand the field operators in the form

$$\begin{aligned}\psi(x)&=\sum_r a_r U_r(x)+\sum_s b_s^\dagger V_s(x),\\ \psi^\dagger(x)&=\sum_r a_r^\dagger U_r^\dagger(x)+\sum_s b_s V_s^\dagger(x)\end{aligned} \tag{12}$$

with *anticommuting* creation and annihilation operators such that

$$\{a_r^\dagger,\,a_{r'}\}=\delta_{r,r'},\quad \{b_s^\dagger,\,b_{s'}\}=\delta_{s,s'}. \tag{13}$$

All other anticommutators vanish. If we set the *equal-time anticommutator* of the field operators $\psi^\dagger(x)$, $\psi(x)$ to be

$$\{\psi(ct,\boldsymbol{x}),\tilde{\psi}(ct,\boldsymbol{y})\}=\gamma^0\delta^3(\boldsymbol{x}-\boldsymbol{y}) \tag{14}$$

where $\tilde{\psi}(x)=\psi^\dagger(x)\gamma^0$; then

$$\sum_r u_r(ct,\boldsymbol{x})u_r^\dagger(ct,\boldsymbol{y})+\sum_s v_s(ct,\boldsymbol{x})v_s^\dagger(ct,\boldsymbol{y})=\delta^3(\boldsymbol{x}-\boldsymbol{y}) \tag{15}$$

so that the complete spectrum of the Dirac free particle field operator has both positive and negative energy solutions. The formalism implies that electrons and positrons obey Fermi statistics: there can be only one electron in state r or positron in state s. In all physically realistic models, *the electron and positron spectra are quite distinct, although their wave functions satisfy the same Dirac equation.* This formalism makes it possible to think of *separate electron and positron fields.* Then

$$N^e=\sum_r n_r,\quad E^e=\sum_r n_r E_r,\qquad N^p=\sum_s n_s,\quad E^p=\sum_s n_s E_s,, \tag{16}$$

are respectively the total number and total energy of the quanta of the electron and positron fields. The combined totals are

$$N=N^e+N^p,\qquad E=E^e+E^p.$$

This construction can also be used with minimal coupling to an external electromagnetic field, $a_\mu(x)$, so that

$$(\gamma^\mu(i\partial_\mu-ea_\mu/c)+\beta c^2)\,\psi(x)=0,\quad a_\mu=(c\phi(\boldsymbol{x}),\boldsymbol{a}(\boldsymbol{x})). \tag{17}$$

The electron field and the positron fields are again in separate domains. The charge conjugation symmetry is broken in an atomic environment as shown schematically in Figure 1.

As it stands, quantization is independent of the particular method of solution of the Dirac equation. Figure 1 illustrates schematically the symmetry of the *free fermion levels* n^+ and n^- about the relativistic energy zero. The charge conjugation operator, C of §3.3.2, sets up a bijective mapping between the n^+ and n^- energy states of *free fermions.* This *symmetry is broken in the atomic or molecular environment*; all realistic physical models identify separate electron and positron domains, which we can think of as defining separate quantum fields although the wave functions are solutions of the same Dirac equation.

Preprints (www.preprints.org) | NOT PEER-REVIEWED | Posted: 18 July 2022 doi:10.20944/preprints202207.0266.v1

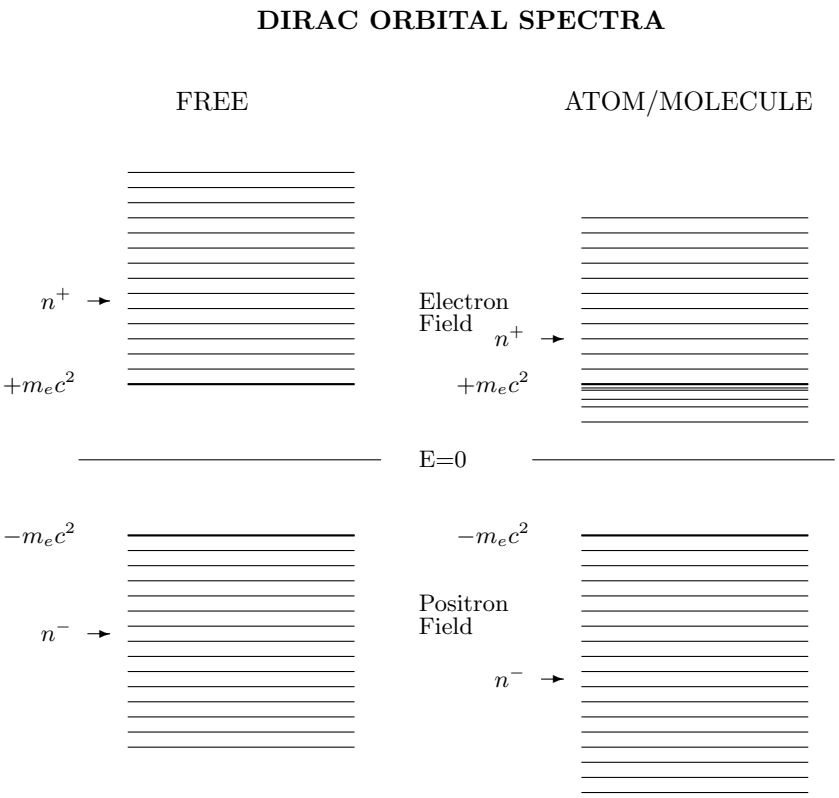

Figure 1: Schematic spectra from CK-spinor calculations. Charge conjugate pairs of energies labelled n^+ and n^- with positions $n^+ = n^-$ and energies $E_{n^+,\kappa} = -E_{n^-,\kappa}$ are lowered by an attractive atomic or molecular potential, breaking the charge conjugation symmetry.

3.3 Basis set spinor expansions

The formalism in current use for solving relativistic atomic and molecular structure problems using a linear combination of spinor basis functions is surveyed in [5, Section 5.6-5.11]. An orbital a in subshell A having the structure (2) is approximated by

$$\psi_a(\boldsymbol{x}) = \begin{pmatrix} \sum_{\mu=1}^{N} c^+_{\mu,a} M[+,\mu;\boldsymbol{x}] \\ \sum_{\mu=1}^{N} c^-_{\mu,a} M[-,\mu;\boldsymbol{x}] \end{pmatrix} \tag{18}$$

where μ labels the large- and small-component basis spinors, $M[\pm,\mu;\boldsymbol{x}]$, which in a molecule may be centred on more than one nucleus. The time-independent

Preprints (www.preprints.org) | NOT PEER-REVIEWED | Posted: 18 July 2022 doi:10.20944/preprints202207.0266.v1

Dirac Hamiltonian for an electron can be written as in (11)

$$\tilde{h}_D = \mathcal{K} + \mathcal{M} + \mathcal{V}, \quad \mathcal{K} = c\boldsymbol{\alpha}\cdot\boldsymbol{p}, \quad \mathcal{M} = \beta mc^2, \quad \mathcal{V} = V(\boldsymbol{x}) \tag{19}$$

where the potential $V(\boldsymbol{x})$ may include interactions with all other charged particles. We can now form a Rayleigh quotient by taking the expectation of $\tilde{h}_D$ with respect to $\psi_a(\boldsymbol{x})$:

$$\mathcal{R} = \langle \boldsymbol{c}_a^\dagger \boldsymbol{H} \boldsymbol{c}_a\rangle / \langle \boldsymbol{c}_a^\dagger \boldsymbol{S} \boldsymbol{c}_a\rangle, \qquad \boldsymbol{c}_a = \begin{pmatrix} \boldsymbol{c}_a^+ \\ \boldsymbol{c}_a^- \end{pmatrix}, \tag{20}$$

where the elements of the N-vectors $\boldsymbol{c}_a^\pm$ are the expansion coefficients of (18),

$$\boldsymbol{H} = \begin{pmatrix} mc^2\boldsymbol{S}^{++} + \boldsymbol{V}^{++} & c\boldsymbol{K}^{+-} \\ c\boldsymbol{K}^{-+} & -mc^2\boldsymbol{S}^{--} + \boldsymbol{V}^{--} \end{pmatrix}, \quad \boldsymbol{S} = \begin{pmatrix} \boldsymbol{S}^{++} & 0 \\ 0 & \boldsymbol{S}^{--} \end{pmatrix}$$

The $N \times N$ matrices $\boldsymbol{K}^{\beta,\beta'} = \boldsymbol{K}^{\beta',\beta\,\dagger}, \boldsymbol{V}^{\beta,\beta}, \boldsymbol{S}^{\beta,\beta}$ have elements

$$\begin{aligned} S_{\mu\nu}^{\beta\beta'} &= \delta_{\beta\beta'} \int M[\beta,\mu;\boldsymbol{x}]^\dagger M[\beta',\nu;\boldsymbol{x}]\, d\boldsymbol{x} \\ V_{\mu\nu}^{\beta\beta'} &= \delta_{\beta\beta'} \int M[\beta,\mu;\boldsymbol{x}]^\dagger\, V(\boldsymbol{x})\, M[\beta',\nu;\boldsymbol{x}]\, d\boldsymbol{x} \\ K_{\mu\nu}^{\beta\beta'} &= \delta_{\beta,-\beta'} \int M[\beta,\mu;\boldsymbol{x}]^\dagger\, \boldsymbol{\sigma}\cdot\boldsymbol{p}\, M[-\beta,\nu;\boldsymbol{x}]\, d\boldsymbol{x} \end{aligned}$$

so that the matrix $\boldsymbol{H}$ is Hermitian. The Rayleigh-Ritz variational method gives Galerkin equations

$$\begin{pmatrix} (mc^2 - E)\boldsymbol{S}^{++} + \boldsymbol{V}^{++} & c\boldsymbol{K}^{+-} \\ c\boldsymbol{K}^{-+} & (-mc^2 - E)\boldsymbol{S}^{--} + \boldsymbol{V}^{--} \end{pmatrix} \begin{pmatrix} \boldsymbol{c}^+ \\ \boldsymbol{c}^- \end{pmatrix} = 0. \tag{21}$$

This generalized eigenvalue equation for $2N$ eigenvalues and eigenfunctions requires basis 4-spinors to have specific relations between its components to give physically useful results. Following (2), we assume

$$M[+,\mu;\boldsymbol{x}] = [f_\kappa^+(r)/r].\,\chi_{\kappa,m}(\theta,\varphi), \quad M[-,\mu;\boldsymbol{x}] = i[f_\kappa^-(r)/r].\chi_{-\kappa,m}(\theta,\varphi). \tag{22}$$

The *kinetic matching* restriction [5, Sec. 5.7] of the radial components

$$f_\kappa^-(r) = \frac{1}{2mc}\left(\frac{d}{dr} + \frac{\kappa}{r}\right) f_\kappa^+(r) \tag{23}$$

ensures that the matrix $\boldsymbol{H}$ reduces to the corresponding $N \times N$ Schrödinger matrix with respect to the radial functions $f_\kappa^+(r)$ in the nonrelativistic limit. More specifically, this construction - we refer to [5, Chap. 5] for the details - gives the nonrelativistic kinetic energy matrix [5, Eq. (5.7.13)]

$$\boldsymbol{T}_{nr}^{++} = \boldsymbol{K}^{+-}(\boldsymbol{S}^{--})^{-1}\boldsymbol{K}^{-+} = \boldsymbol{S}^{--}, \tag{24}$$

so that (21) reduces to the matrix Schrödinger equation

$$[\boldsymbol{T}_{nr}^{++} + \boldsymbol{V}^{++} - \epsilon\boldsymbol{S}^{++}]\boldsymbol{c}^+ = 0. \tag{25}$$

where $\epsilon = E - mc^2$ is the eigenvalue relative to the nonrelativistic zero of energy. Note that kinetic matching is not a relativistic effect. It is a consequence of the structure of the Dirac operator, essential for ensuring correct behaviour in the nonrelativistic limit. Successful types of kinetically matched spinor basis functions are listed in [5, Sec. 5.8-5.10] along with numerical examples.

Preprints (www.preprints.org) | NOT PEER-REVIEWED | Posted: 18 July 2022 doi:10.20944/preprints202207.0266.v1

3.3.1 KG-spinors

The fact that the upper ("large") radial component of a 4-spinor may be of any form used in nonrelativistic atomic models defines the class of K-spinors in which the radial components are related by (23). We consider only the Gaussian (KG-spinor) sets, from which the BERTHA relativistic molecular program [8] is built:

$$f^{+}_{\kappa,i}(r) = \begin{cases} r^{K}\, e^{-\lambda_{K,i} r^2}, & \kappa = -K \\ r^{K+1}\, e^{-\lambda_{K,i} r^2}, & \kappa = +K \end{cases} \tag{26}$$

where the exponents are $\lambda_{K,i} = \alpha\beta^{i-1}, i = 1, 2, \ldots, N$ with suitable chosen parameters α, β, N that may depend on $K = |\kappa|$. From (23), the lower components are

$$f^{-}_{\kappa,i}(r) = \begin{cases} C_{\kappa,i}\; r^{K+1}\, \lambda_{K,i}\, e^{-\lambda_{K,i} r^2}, & \kappa = -K \\ C_{\kappa,i}\; r^{K}\, e^{-\lambda_{K,i} r^2}\, \left((2K+1) - 2\lambda_{K,i} r^2\right), & \kappa = +K \end{cases} \tag{27}$$

where $C_{\kappa,i}$ are arbitrary constants, chosen to enforce normalization. KG-spinors have been shown to give excellent results for atomic and molecular structure and properties but they lack the symmetry needed to give a balanced representation of positron states.

3.3.2 Charge conjugation

The charge conjugation matrix C sets up a bijective mapping between the elements of the domains of *free electrons and positrons* whose importance in atomic and molecular structure calculations has hitherto been neglected. The *charge conjugation mapping* is

$$\psi \to \psi_c = C\overline{\psi}^{t}, \qquad C = i\gamma^2\gamma^0 = \begin{pmatrix} 0 & -i\sigma^2 \\ -i\sigma^2 & 0 \end{pmatrix}, \quad C^t = C^\dagger = -C, \tag{28}$$

where $\overline{\psi}^{t} = \psi^*\gamma^0$ is Dirac conjugation[2]. Minimal coupling of a particle with charge q to an external electromagnetic field a_μ replaces (8) by

$$(i\gamma^\mu\partial_\mu - mc)\psi(x) = \frac{q}{c}\gamma^\mu a_\mu\, \psi(x). \tag{29}$$

A simple calculation shows that

$$(i\gamma^\mu\partial_\mu - mc)\psi_c(x) = -\frac{q}{c}\gamma^\mu a_\mu\, \psi_c(x). \tag{30}$$

so that charge conjugation reverses the sign of the particle's charge. The expectation value of an operator $\mathcal{O}$ is given by

$$\langle\mathcal{O}\rangle = \int \overline{\psi}\,\mathcal{O}\,\psi\, d^3x, \quad \langle\mathcal{O}\rangle_c = \int \overline{\psi}_c\,\mathcal{O}\,\psi_c\, d^3x, \tag{31}$$

[2]The asterisk denotes complex conjugation, and the superscript t denotes vector transposition

Preprints (www.preprints.org) | NOT PEER-REVIEWED | Posted: 18 July 2022 doi:10.20944/preprints202207.0266.v1

so that for *free particles* we have

$$\langle x^\mu\rangle_c = \langle x^\mu\rangle, \quad \langle p^\mu\rangle_c = -\langle p^\mu\rangle, \quad \langle j^\mu\rangle_c = -\langle j^\mu\rangle,$$
$$\langle \boldsymbol{\Sigma}\rangle_c = -\langle \boldsymbol{\Sigma}\rangle, \quad \langle \boldsymbol{L}\rangle_c = -\langle \boldsymbol{L}\rangle, \quad \langle \boldsymbol{J}\rangle_c = -\langle \boldsymbol{J}\rangle,$$

These electron/positron symmetry relations are broken by interaction with other particles in atoms and molecules. Figure 1 compares the spectrum of the Dirac operator for free particles on the left, with a typical atomic potential on the right, generated using a basis set which respects free particle charge conjugation. The free spectrum is symmetric about energy $E = 0$, while the atomic potential lowers all eigenvalues, introducing bound states and making $E_{n^+} \neq -E_{n^-}$.

Atomic and molecular structure calculations write the Dirac Hamiltonian in the form

$$H_D(q) := c\boldsymbol{\alpha}\cdot(\boldsymbol{p} - q\boldsymbol{A}) + \beta mc^2 + q\phi \tag{32}$$

so that for particles of charge q

$$\langle H_D(q)\rangle_c = -\langle H_D(-q)\rangle. \tag{33}$$

The standard 4-spinor in spherical coordinates with real radial amplitudes $f_\kappa^\beta(r)$ has the form

$$\psi_{\kappa,m}(\boldsymbol{x}) = \frac{1}{r}\begin{pmatrix} f_\kappa^+(r)\,\chi_{\kappa m}(\theta,\varphi) \\ i f_\kappa^-(r)\,\chi_{-\kappa m}(\theta,\varphi)\end{pmatrix}; \tag{34}$$

applying (28) gives the charge conjugate spinor

$$\psi_{-\kappa,-m}(\boldsymbol{x})_c = -i(-1)^{m+1/2}\frac{1}{r}\begin{pmatrix} f_\kappa^-(r)\,\chi_{-\kappa,-m}(\theta,\varphi) \\ i f_\kappa^+(r)\,\chi_{\kappa,-m}(\theta,\varphi)\end{pmatrix}. \tag{35}$$

3.3.3 CKG-spinors

CKG-spinors are derived by adding a charge conjugate symmetric set to a basis of radial KG-spinors:

$$\psi(\boldsymbol{x}) = \sum_\alpha \sum_\mu c_{\mu,\alpha} G^\alpha[\mu;\boldsymbol{x}] \tag{36}$$

where $G^\alpha[\mu;\boldsymbol{x}]$ is a four-component KG-spinor basis function; $\alpha = \pm 1$ denotes positive- and negative-energy respectively, and setting $\mu = \{\kappa, m, i\}$,

$$G^\pm[\kappa,m,i;\boldsymbol{x}] = N^\pm_{\kappa,i}\begin{pmatrix} P^\pm_{\kappa,i}(r)\chi_{\kappa,m}(\theta,\varphi) \\ i\,Q^\pm_{\kappa,i}(r)\chi_{-\kappa,m}(\theta,\varphi)\end{pmatrix} \tag{37}$$

with normalisation constants $N^\pm_{\kappa,i}$. For positive energies ($\alpha = +1$), the explicit radial components using (23) are

$$P^+_{-K,i}(r) = r^K \exp[-\lambda_{K,i} r^2] \tag{38}$$
$$Q^+_{-K,i}(r) = (c + E_{-K,i}/c)^{-1}(-2\lambda_{K,i} r^{K+1})\exp[-\lambda_{K,i} r^2]$$

$$P^+_{+K,i}(r) = r^{K+1} \exp[-\lambda_{|K,i} r^2] \tag{39}$$
$$Q^+_{+K,i}(r) = (c + E_{+K,i}/c)^{-1}(2K + 1 - 2\lambda_{K,i} r^2) r^K \exp[-\lambda_{K,i} r^2].$$

Preprints (www.preprints.org) | NOT PEER-REVIEWED | Posted: 18 July 2022 doi:10.20944/preprints202207.0266.v1

Charge conjugation symmetry makes the construction of negative energy radial basis functions simple:

$$P^{\pm}_{\kappa,i}(r) = Q^{\mp}_{-\kappa,i}(r), \quad N^{\pm}_{\kappa,i} = N^{\mp}_{-\kappa,i}. \tag{40}$$

The parameter $E_{\pm K,i}$, corresponds to the magnitude of the average free-particle energy. In the so-called "dual kinetic balance" basis [15], this parameter is simply set to c^2, on the grounds that we are mainly interested in positive energy bound-states. As high-energy states play a significant role in QED correction calculations, we choose

$$E_{\pm K,i} = +c\sqrt{\langle p^2_{\pm K,i}\rangle + c^2} \tag{41}$$

where

$$\langle p^2_{-K,i}\rangle = (2K+3)\lambda_{K,i}, \quad \langle p^2_{+K,i}\rangle = (2K+1)\lambda_{K,i}$$

The normalization constants, $N^{\pm}_{\kappa,i}$, are chosen so that

$$\int_0^{2\pi} d\varphi \int_0^{\pi} \sin\vartheta d\vartheta \int_0^{\infty} r^2 dr \; G^{\pm\dagger}[\kappa,m,i]G^{\pm}[\kappa,m,i] = 1$$

for all valid κ and m.

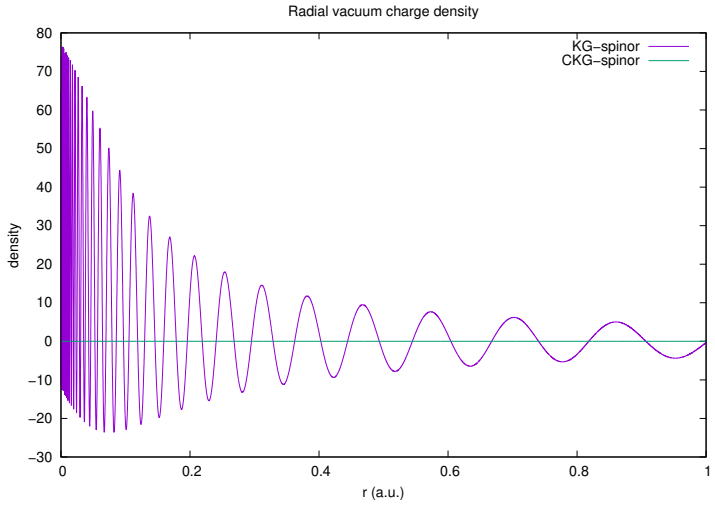

Figure 2: Comparison of KG- and CKG-spinor representations of the radial vacuum charge density from free electron/positron states with $K = 1$ only. The calculations were performed in both cases using a geometric sequence of exponents, $\lambda = \alpha\beta^{i-1}, i = 1, 2, \ldots, N$, where $\alpha = 0.01$, $\beta = 1.5$ and $N = 50$.

Figure 2 vividly illustrates the necessity of charge conjugation symmetry in a calculation of the $K = 1$ contribution to the vacuum charge density. The rapid oscillations of the KG-spinor radial density integrate to zero, whilst the CKG-spinor calculation radial densities cancel within rounding errors for all radii by

Preprints (www.preprints.org) | NOT PEER-REVIEWED | Posted: 18 July 2022 doi:10.20944/preprints202207.0266.v1

construction. This ensures charge and parity conservation in interaction matrix elements.

Table 1 reports eigenvalues of a test calculation on the hydrogenic ion Hg^{+79} obtained with a large CKG-spinor basis. The exponents for all values of $K = |\kappa|$ were $\lambda_{K,i} = \alpha\beta^{i-1}\{i = 1, 2, \ldots, 100\}$ with $\alpha = 0.001$, $\beta = 1.40$. The table reports only the first three numerical eigenvalues of each symmetry κ together with the lowest exact analytic eigenvalue. The first two columns agree to 10 decimal places for all κ with the minor exception of the first two lines $|\kappa| = 1$. Notice 10 decimal hydrogenic eigenvalue agreements such as between $2s_{1/2}(E_{n_2,-1})$ and $2p_{1/2}(E_{n_1,1})$.

As with KG-spinors, the negative energy solutions all have energies below the line $E = -mc^2$.

Table 1: CKG-spinor calculation of eigenvalues (a.u.), relative to the nonrelativistic zero of energy, of Hg^{79+} with a point nucleus. Exact Bohr-Sommerfeld eigenvalues in the second column, followed by computed eigenvalues (units E_h) for the three lowest bound states of each symmetry κ in order.

κ	$E_{Analytic}$	$E_{n_1,\kappa}$	$E_{n_2,\kappa}$	$E_{n_3,\kappa}$
-1	-3532.1921489294	-3532.1921489289	-904.8478012876	-392.0836928780
1	-904.8478012882	-904.8478012878	-392.0836928781	-216.4247478039
-2	-817.8074977480	-817.8074977480	-366.1427114567	-205.5771277760
2	-366.1427114567	-366.1427114567	-205.5771277760	-131.1010555098
-3	-358.9868485160	-358.9868485160	-202.5363034958	-129.6328330777
3	-202.5363034958	-202.5363034958	-129.6328330776	-89.9621990162
-4	-201.0765233582	-201.0765233582	-128.8823613985	-89.5273365309
4	-128.8823613985	-128.8823613985	-89.5273365309	-65.7655876909
-5	-128.4392341889	-128.4392341889	-89.2702733629	-65.6035374887
5	-89.2702733629	-89.2702733629	-65.6035374887	-50.2279904000
-6	-89.1002663743	-89.1002663743	-65.4963124418	-50.1561023779
6	-65.4963124418	-65.4963124419	-50.1561023780	-39.6314776684
-7	-65.4200746697	-65.4200746697	-50.1049761176	-39.5955492450
7	-50.1049761176	-50.1049761176	-39.5955492450	-32.0742810655
-8	-50.0667420260	-50.0667420260	-39.5686766900	-32.0546823612
8	-39.5686766900	-39.5686766900	-32.0546823613	-26.4929690886
-9	-39.5478161969	-39.5478161969	-32.0394670086	-26.4815336906
9	-32.0394670087	-32.0394670087	-26.4815336906	-22.2529707815
-10	-32.0273112566	-32.0273112566	-26.4723972662	-22.2459315332
10	-26.4723972662	-26.4723972662	-22.2459315332	-18.9559506743

4 QED corrections

4.1 Vacuum Polarization

A long-standing ambition has been to evaluate numerically on the fly the contribution of vacuum polarization to orbital energies for each atomic state. CKG-spinors defined in Sec. 3.3.3 make this possible. This is because we can diago-

Preprints (www.preprints.org) | NOT PEER-REVIEWED | Posted: 18 July 2022 doi:10.20944/preprints202207.0266.v1

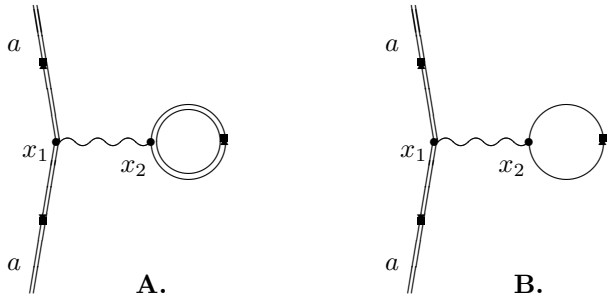

Figure 3: Vacuum polarization diagrams. Double lines indicate electron propagation in the external field; single lines correspond to free particle propagation. The observed effect is given entirely by diagram A: external field propagation of virtual electrons and positrons in the loop breaks charge conjugation symmetry. The contribution of free virtual electrons and positrons in the loop of diagram B cancels identically by Furry's Theorem.

nalize the Dirac Hamiltonian

$$h_Z = h_0 - Z/r$$

for all Z in terms of a common basis, simplifying evaluation of the matrix elements appearing in equations (42) and (43) below. The principle of this calculation was demonstrated by Persson *et al.* [16] who used a similar technology based on partial wave expansion to evaluate the Wichmann-Kroll potential [17]. They started from the Feynman diagram, Figure 3, expanding the photon propagator in partial waves is [16, Eq. 2.6]

$$U_{VP}(\boldsymbol{x}_1) = -\frac{ie^2}{4\pi\epsilon_0}\frac{2}{\pi}\int d^3\boldsymbol{x}_2 \int_0^\infty dk \int_{-\infty}^\infty \frac{dz}{2\pi}\sum_{l=0}^\infty (2l+1) j_l(kr_1)\, \boldsymbol{C}^l(1)\alpha^\mu(1) \times \sum_t \frac{\Phi_t^\dagger(\boldsymbol{x}_2) j_l(kr_2)\, \boldsymbol{C}^l(2)\alpha_\mu(2)\Phi_t(\boldsymbol{x}_2)}{z - E_t(1-i\eta)}. \tag{42}$$

Any vacuum polarization acting on the electron in atomic orbital a is due to the closed loop in which electrons circulate in one direction and positrons in the other. In Figure 3B the currents cancel by charge conjugation symmetry so that the photon has zero energy; the external field breaks the charge conjugation symmetry of electrons and positrons as illustrated in Figure 1 so that the exchanged photon in Figure 3A has a finite energy[3]. Equation (42) can be simplified giving

$$U_{VP}(r) = -\frac{e^2}{4\pi\epsilon_0}\frac{1}{\pi}\int_0^\infty dk\, j_0(kr)\sum_\kappa (2j_\kappa + 1) \times \sum_n \mathrm{sgn}(E_{n\kappa,Z})\langle n\kappa, Z\,|j_0(kr_2)|\, n\kappa, Z\rangle. \tag{43}$$

where the index t in (42)has been replaced by n. The summation over n includes the complete set of radial functions for each κ. The case $Z = 0$ applies to freely

[3]Schweber [18, p. 571, Section 15g] makes this point in a review of the Furry Picture

Preprints (www.preprints.org) | NOT PEER-REVIEWED | Posted: 18 July 2022 doi:10.20944/preprints202207.0266.v1

moving electrons, and it is easy to show that pairs of matrix elements related by charge conjugation symmetry cancel. This symmetry is broken when $Z > 0$.

Figure 2 has already demonstrated that the CKG-spinor result for the zero potential term, $Z = 0$, is consistent with Furry's theorem. We can also use the CKG-spinors to evaluate the unrenormalized one-potential term:

$$V_0^{(1)}(\boldsymbol{r_1}) = -\frac{e^2}{4\pi\epsilon_0}\frac{4}{\pi}\int_0^\infty dk\, j_0(kr_1)\sum_\kappa (2j_\kappa+1) \times \sum_p^+ \sum_q^- \frac{\langle p\kappa,0\,|j_0(kr)\,|\,q\kappa,0\rangle\,\langle q\kappa,0\,|\,Z\,|\,p\kappa,0\rangle}{E_{p\kappa,0}-E_{q\kappa,0}}, \tag{44}$$

using the free particle Dirac Hamiltonian, $Z = 0$, to evaluate the kets $|p\kappa,0\rangle$ and free particle eigenvalues $E_{p\kappa,0}$. CKG-spinor evaluation of the matrix elements $\langle p\kappa,0\,|j_0(kr)\,|\,q\kappa,0\rangle$ is straightforward. Alternatively, we can use free electron partial waves whose radial amplitudes are proportional to spherical Bessel functions, giving matrix elements proportional to the vertex integrals, Section 6.

Table 2 compares partial wave contributions to the $1s$ vacuum polarization in Hg^{79+} with a point nucleus. The first column is the CKG-spinor contribution from (43) using atomic spinors with $Z = 80$. Column 2 shows the corresponding one-potential contribution from (44) with the $|p\kappa,0\rangle$ generated in the same CKG-spinor basis. Following [16], we interpret the difference in the last column as the contribution of Wichmann-Kroll and higher order contributions. Table 3 compares the literature values [20] of the Wichmann-Kroll contribution for a range of values of Z with the corresponding CKG-spinor calculation. The third column corresponds (for $Z = 80$) to the extrapolated total in the last column of Table 2.

Table 2: Partial wave contributions to $\langle 1s\,|U_{VP}|\,1s\rangle$ in Hg^{79+}. The CKG-spinor exponents are $\lambda_i = \alpha\beta^{i-1}\{i = 1, 2, \ldots N\}$, with $\alpha = 0.1, \beta = 1.9, N = 90$

$K = \lvert\kappa\rvert$	$\langle V_{Z,K}\rangle$	$\langle V^{(1)}_{0,K}\rangle$	$\langle V_{Z,K}\rangle - \langle V^{(1)}_{0,K}\rangle$
1	3.29166528	3.22434547	6.73198 (-2)
2	2.81964973	2.81325408	6.39565 (-3)
3	2.40679616	2.40522784	1.56831 (-3)
4	2.07156051	2.07095146	6.09053 (-4)
5	1.79881093	1.79850086	3.10045 (-4)
6	1.57229887	1.57211452	1.84348 (-4)
7	1.38083155	1.38071232	1.29222 (-4)
8	1.21719228	1.21711175	8.05279 (-5)
Sum	16.5588053	16.42822183	7.65869 (-2)

We have not yet been able to make comparisons with extensive calculations such as those of Sapirstein and Cheng [21], who used a coordinate space formalism to calculate vacuum polarization energies for hydrogenic ions with finite size nuclei and principal quantum numbers $n = 1, \ldots, 5$. They also calculated results for lithium-, sodium- and copper-like ions using Kohn-Sham potentials

Preprints (www.preprints.org) | NOT PEER-REVIEWED | Posted: 18 July 2022 doi:10.20944/preprints202207.0266.v1

Table 3: Comparison of Wichmann-Kroll contribution to vacuum polarization of hydrogenic $1s_{1/2}$ electrons [20] with CKG-spinor results.

Z	$\langle V^{WK}\rangle$ [20]	$\langle V_0^{(3)}\rangle$	$\langle V_0^{(3+)}\rangle$
10	0.3232201E-06	0.3740969E-06	0.3714822E-06
20	0.1862744E-04	0.2036149E-04	0.2042291E-04
30	0.1964703E-03	0.2093781E-03	0.2114400E-03
40	0.1046683E-02	0.1098815E-02	0.1120773E-02
50	0.3869888E-02	0.4023198E-02	0.4158461E-02
60	0.1144670E-01	0.1181736E-01	0.1242842E-01
70	0.2926072E-01	0.3005133E-01	0.3230899E-01
80	0.6784298E-01	0.6935930E-01	0.7667064E-01

and first-order screening corrections. These are brute force computations. They found it necessary to use an extremely fine radial grid of up to 50,000 points when calculating electron wave functions to control the accuracy of the photon energy integration, where they encounter numerical instabilities giving unphysical behaviour at very high energies $\omega \approx 10^6 mc^2$ or greater.

5 Electron self-energy

There seems no reason why charge symmetric CK-spinors should not be equally useful in calculating the electron self-energy correction, orders of magnitude larger than the vacuum polarization correction, to atoms and molecules. The partial wave renormalization approach was developed in [22, 23] and, with rather different technology, in [16]. The *partial wave expressions* to be evaluated for the self-energy of a bound orbital a can be reduced to the general form

$$E_\kappa(a) = 2\pi\alpha \int \frac{d^3k}{(2\pi)^3}\,\frac{1}{k}\sum_n \frac{\langle a|\alpha_\mu e^{-i\boldsymbol{k}\,\cdot\,\boldsymbol{x}}|n\kappa,Z\rangle\,\langle n\kappa,Z|\alpha^\mu e^{i\boldsymbol{k}\,\cdot\,\boldsymbol{x}}|a\rangle}{E_a - E_{n\kappa,Z} - ck\,\mathrm{sgn}(E_{n\kappa,Z})} \tag{45}$$

where the sum over intermediate virtual states $|n\kappa,Z\rangle$ runs over the complete Dirac spectrum. The integrand is finite for each $|n\kappa,Z\rangle$, but *the partial wave sum over κ diverges logarithmically* whether for free ($Z=0$) or bound ($Z>0$) sums [22, Table 1]. We write $E_\kappa(a) = M_\kappa(a)$ when the intermediate states are free, $Z=0$, and $E_\kappa(a) = B_\kappa(a)$ for $Z>0$. The divergent sum $M(a) = \sum_\kappa M_\kappa(a)$, the *renormalization counter term*, is usually interpreted as already forming part of the observed mass of the electron. Partial wave renormalization amounts to calculating the convergent sum $E(a) = \sum_\kappa R_\kappa(a)$, where $R_\kappa(a) = B_\kappa(a) - M_\kappa(a)$ [22, Table 2]. Charge conjugation symmetry breaking is the obvious explanation of the physical effect, much as in vacuum polarization.

The use of CK-spinors for self-energy has still to be investigated. The results of [22, 23] for $Z>0$ used a Wick rotation, $k_0 \to i\omega$, for the configuration space propagator in (45) similar to that used by Sapirstein and Cheng [21] in their work on vacuum polarization. The counter terms $M_\kappa(a)$ treated the bound state as a wave packet superposition of free states of the same symmetry κ_a:

Preprints (www.preprints.org) | NOT PEER-REVIEWED | Posted: 18 July 2022 doi:10.20944/preprints202207.0266.v1

$|a\rangle = \sum_n |n\kappa_a, 0\rangle \langle n\kappa_a, 0|a\rangle$, so that the matrix elements in the numerator of (45) are proportional to the free electron vertex integrals of Section 6. The different algorithms all give similar accuracy.

6 Vertex integrals

The Feynman diagrams of QED visualize interaction processes of free electron and positron quanta with photons. When these quanta are expressed in partial waves, the amplitude at each interaction vertex of the diagram is proportional to an integral [24] defined by

$$I_{l,_f,l_i}(k, p_f, p_i) = \frac{4kp_fp_i}{\pi} \int_0^\infty j_l(kr)\, j_{l_f}(p_f r)\, j_{l_i}(p_i r)\, r^2\, dr. \tag{46}$$

where the $j_l(x)$ are spherical Bessel functions. These have important properties [24]:

1. $I_{l,_f,l_i}(k, p_f, p_i)$ is non-zero if and only if orbital angular momentum is conserved at the vertex: $|l_f - l_I| \le l \le l_f + l_i$.
2. $I_{l,_f,l_i}(k, p_f, p_i)$ is non-zero if and only if linear momentum is conserved at the vertex: $|p_f - p_i| \le l \le p_f + p_i$.
3. $I_{l,_f,l_i}(k, p_f, p_i)$ is invariant with respect to simultaneous permutations of the angular momentum labels $\{l, l_f, l_i\}$ and the 3-momenta $\{k, p_f, p_i\}$.
4. For any $\alpha > 0$, $I_{l,l_f,l_i}(k, p_f, p_i) = I_{l,l_f,l_i}(\alpha k, \alpha p_f, \alpha p_i)$ so that the vertex integral depends only on the ratios of the momenta.
5. The number triads $\{l, l_f, l_i\}$ and $\{k, p_f, p_i\}$ must be able to form the lengths of the sides of a plane triangle. Every non-zero vertex integral has a factor

$$\Delta(k, p_f, p_i) = \begin{cases} 1 & \text{if } (k, p_f, p_i) \text{form a non} - \text{degenerate triangle} \\ \frac{1}{2} & \text{if } (k, p_f, p_i) \text{form a degenerate triangle} \\ 0 & \text{otherwise} \end{cases}.$$

6. Special values:

$$\begin{aligned} &I_{0,0,0}(k, p_f, p_i) = \Delta(k, p_f\, p_i) \\ &I_{0,1,1,}(k, p_f, , p_i) = \cos\theta_k = (p_f^2 + p_i^2 - k^2)/2p_fp_i \\ &\lim_{k\to 0} \frac{1}{2k}\, I_{l,l_f,l_i}(k, p_f\, p_i) = \delta(p_f - p_i)\, \delta_{l,0}\, \delta_{l_f,l_i} \\ &\int_0^\infty j_l(kr)\, j_l(k'r)\, r^2\, dr = \frac{\pi}{2kk'}\, \delta(k - k'). \end{aligned}$$

where θ_k is the angle of the triangle opposite side k. The sine rule gives

$$\frac{\sin\theta_k}{k} = \frac{\sin\theta_f}{p_f} = \frac{\sin\theta_i}{p_i}.$$

A recursive algorithm for evaluating vertex integrals is described in [24]

 doi:10.20944/preprints202207.0266.v1

7 Conclusions

The role of symmetry in both atomic and molecular calculations and also in quantum electrodynamics has been central to this paper. QED was formulated [9, 10, 11, 18], when computers were in their infancy and the most advanced computational aids were hand or electric calculators. Relativistic atomic structure programs like GRASP initially adapted algorithms on lines proposed in Hartree's 1957 lectures [3]. The symmetry structure of Dirac spinors on which GRASP is built [4, 5], not yet fully understood in 1957, would not have been possible without the fundamental work of Racah [25] on quantum theory of angular momentum. The effectiveness of K-spinor and CK-spinor basis sets in atomic and molecular calculations required sufficiently powerful computer hardware and software.

Atomic structure models exploit spherical symmetry near a fixed nucleus. Nonrelativistic quantum chemistry with atoms on different centres needed different numerical methods; naive attempts to extend the basis set algorithms of Roothaan [6] and Hall [7] to relativistic quantum chemistry failed catastrophically at first. The introduction of Dirac 4-spinors and kinetic matching [5, p. 292] overcame the problems, eliminating unphysical numerical solutions and unrealistic 'relativistic energies', so that the numerical equations reduced exactly to the equivalent nonrelativistic equations as $c \to \infty$. These developments were enough to encourage the use of basis set methods in relativistic molecular codes like BERTHA, but most atomic codes like GRASP still approximate the wave functions on radial grids.

Most calculations of QED corrections rely on well-established methods originating some 70 years ago applicable to hydrogen-like, or at most helium-like or lithium-like, atoms. Perturbation theory coupling the quantized free electrons and positrons with photons is highly developed. Schweber [10, p. 595] observes 'Renormalization theory is a complicated conceptual system. ... (that) can be viewed as a technical device for circumventing - and discarding - the infinite results that occur in perturbative calculations in quantum field theory.' For this reason, most applications of QED to atomic and molecular structure have tried, not entirely satisfactorily, to adapt numerical data from complex calculations on hydrogenic systems.

CK-spinors with matched charge conjugate basis components now provide a balanced representation of electron and positron wave functions, with the potential to calculate the leading QED corrections as part of a standard atomic or molecular structure calculation. The evaluation of interaction integrals is straightforward and there are no divergent integrals to contend with. The Wichmann-Kroll calculation of [16] uses different basis sets based on solving the Dirac equation in a (large) sphere, but the zero-potential contribution is non-zero and has to be removed. Another coordinate-space approach [26] starts with the same Feynman integral, but assumes that it is divergent and needs regularization to produce a valid functions for analytical or numerical evaluation, introducing Pauli-Villars regularization of the electron Green's function much as described above in Schweber's Epilogue. It is not difficult to conclude that the QED tradition of starting with free electrons and positrons is not well suited to atomic and molecular modelling. Perturbation theory runs rapidly into an analytical and computational morass and has also to cope with divergent integrals. The simplicity of the CK-spinor coordinate-space algorithms deserves to

be more widely used.

We should never forget that a change of viewpoint can suggest new and better ways of doing things.

Author contributions

Conceptualizations: Ian Grant and Harry Quiney

References

[1] https://github.com/compas/

[2] https://compas.github.io

[3] Hartree, D.R. *The calculation of atomic structures* (John Wiley & Sons, Inc., **1957**)

[4] Grant I.P. *Proc.Roy.Soc.A*262, 555-576 (**1961**)

[5] Grant I.P. *Relativistic quantum theory of atoms and molecules: theory and computation* (Springer Science and Business Media, LLC, **2007**)

[6] Roothaan C.C.J. *Rev.Mod.Phys.* **23**, 69 (**1951**); *Rev.Mod.Phys.* **32**, 179 (**1961**)

[7] Hall G.G. *Proc.Roy.Soc. A* **205**, 541 (**1951**)

[8] Belpassi L., de Santis M., Quiney H.M., Tarantelli F. and Storchi L., J. Chem. Phys. **152**, 164118 (2020).

[9] Pais A. *Inward Bound* (Oxford University Press) (**1986**)

[10] Schweber S.S. *QED and the men who made it* (Princeton University Press) (**1994**)

[11] Weinberg S. *Quantum Theory of Fields, Vol 1* (Cambridge University Press) (**1995**)

[12] Dirac P.A.M. *Proc.Roy.Soc. A* **117**, 610; ;. . . *Proc.Roy.Soc. A* **118**, 641 (**1928**)

[13] Gordon W. *Z. Phys.* **48**, 11 (**1928**)

[14] Darwin C.G. *Proc.Roy.Soc. A* **118**, 654 (**1928**)

[15] Shabaev V.M., Tupitsyn I.I., Yerokhin V.A., Plunien G., Soff G.,, Physical Review Letters, **93**, 130405 (2004).

[16] Persson H., Lindgren I., Salomonson S. and Sunnergren P., *Phys. Rev. A* **48**, 2772-2778 **(1993)**.

[17] Wichmann E.H. and Kroll N.M., *Phys. Rev.* **101**, 843. **(1956)**

[18] Schweber S.S., *Relativistic quantum field theory* (New York: Harper and Row) **(1961)**

[19] Feynman R.P., *Phys. Rev.* **76**, 749 **(1949)**; *Phys. Rev.* **76**, 769 **(1949)**

[20] Blomqvist J. 1972 *Nucl. Phys. B* **48**, 95.

[21] Sapirstein J. and Cheng K.T., `arXiv:physics/0308022v1` [physics.atom-ph] 5 Aug 2003 **(2003)**

[22] Quiney H M and Grant I P *J. Phys. B: At. Mol. Opt. Phys.* **27**, L299-L304. **(1994)**

[23] Quiney H.M. and Grant I.P.,*Physica Scripta* **T46** 132–138 **(1993)**

[24] Grant I.P. and Quiney H.M., *J. Phys. A: Math. Gen.* **26**, 7547-7562. **(1993)**

[25] Racah, G., *Phys. Rev.* **62**, 438 (1942); *Phys. Rev.* **63**, 367 (1943); *Phys. Rev.* **76**, 1352 (1949)

[26] Indelicato P., Mohr P.J. and Sapirstein J., *Phys. Rev. A* **89**, 0421221 (2014)